Smart Border Patrol Using Drones and Wireless Charging System under Budget Limitation

Navid Ahmadian[a], Gino J. Lim[a,*], Maryam Torabbeigi[a], Seon Jin Kim[b]

[a]*Department of Industrial Engineering, University of Houston, TX, United States*
[b]*Republic of Korea Army, South Korea*

Abstract

Harsh environmental factors surrounding the national borders as well as their extensive length makes the use of manned systems for monitoring every location on the border a risky, expensive, and hardly possible task. Smart border patrol using small-size drones may provide significant help in patrolling areas inaccessible to patrol agents, reduce agent response time, and increase the safety of patrol agents working in dangerous regions. However, the short flight duration associated with small-size drones due to battery limitation can be a serious drawback for such a system for a seamless surveillance. Therefore, this paper proposes a drone-based continuous surveillance system for border patrol with a dynamic wireless battery charging system that is built onto electrification line (E-line). To control the maximum time interval between two consecutive flights to a particular section of the border, a permitted revisiting gap is assigned to each location on the border based on its criticality. A multi-objective mixed-integer non-linear programming (MINLP) model is developed to minimize both the total length of the E-line system for the wireless charging system and the number of drones to satisfy the revisiting gap constraint for a secure border patrol. A solution algorithm is proposed to achieve the Pareto-optimal set. This method provides the decision-maker with a set of candidate solutions to choose from based on their priorities and budgetary constraints-. We illustrate our method using a case study on a segment of the US-Mexico borderline.

Keywords: Smart Border Patrol, Border Surveillance, Drones, Wireless Charging System

1. Introduction

Unmanned Aerial Vehicles (UAVs), commonly known as "drones," are becoming a more accessible alternative to performing tasks that are usually operated by crewed vehicles. Drones have applications in various areas such as delivery [8, 29, 28], damage assessment [24, 27], search and rescue [3, 25], healthcare [17], military purposes [20, 26], and border surveillance [1, 7, 11]. Accommodating cameras, sensors, and other information gathering equipment allow drones the

*Corresponding Author
Email addresses: nahmadian@uh.edu (Navid Ahmadian), ginolim@uh.edu (Gino J. Lim), maryam.torabbeigi@gmail.com (Maryam Torabbeigi), sonjin64@gmail.com (Seon Jin Kim)

opportunity to provide high-quality information about the surveilled area. Hence, drones can be of significant help in monitoring areas where human intervention is risky, expensive, or hardly possible. Specifically, in response to tough environmental factors posed within national border areas, drones can facilitate border monitoring by simultaneously allowing fewer agent deployment and maintaining counter intrusion detection [11]. Drones can fill the gap in the current border surveillance system by 1) improving coverage along remote sections, 2) providing real-time information to the control-operator for quicker response, and 3) reducing the risk of agent endangerment.

The use of drones for border surveillance began in 1990 along the U.S.-Mexico border in Texas [33]. The goal of the mission was drug interdiction [19]. Since 2005, U.S. Customs and Border Protection (CBP) has operated a version of the military drone, Predator B, along the border [12]. From 2013 to 2016, Predator B was operated a total of approximately 5,000 hours per year, which was only around 7% of the total available hours needed for border monitoring [6]. These types of drones are very powerful but are also very expensive. Hence, using such drones is not applicable for arranging highly frequent flights to every location on the border. As an alternative, small-size drones with multi-rotors are less expensive and a large number of them can be used to perform frequent flights to each segment of the border.

Despite the potential benefits of using small-size drones for border patrol, there are some challenges to overcome before they are fully adopted for border surveillance systems. One of these issues includes drone battery limitation and its burdensome recharging process [10, 13, 15]. Most small-size drones in the market currently have flight limitations capped at about half an hour, thus requiring a frequent swap or recharge of the drone battery in the middle of the surveillance mission.

There exist some approaches to addressing the battery limitation issue in the literature. Using fuel cell battery systems are said to improve the endurance of the battery and increase the drone's flight time [9, 14]. However, fuel cells are too heavy for the small-size drone to operate efficiently. Another approach is to use solar power to recharge the drone's battery [4, 18]. The issue with using solar panels is that the energy harvest is inefficient and installing them on small-size drones may not be practical. Several studies have considered swapping either the drone's battery or the drone itself in the midst of an operation [10, 21, 31], which can indubitably extend the flight duration of the drone. However, this method presents two issues: 1) operation cost is increased due to the need to administer additional drones and batteries, and 2) drones would be required to more frequently return to the depots for battery swapping. Therefore, using these approaches do not adequately support a non-stop flight for the drones while they monitor the border. Contrarily, some studies in the literature suggest the use of a wireless charging system for the drones as another, distinct solution to the battery limitation problem posed [30, 32]. In this paper, we implement the wireless charging approach to achieve a non-stop drone operation.

Although drones have been the subject of many studies, few studies have focused on the implementation of the drone for border surveillance. A drawback of using small drones for continuous surveillance is the flight time limitation due to the current battery technology. To address this issue, Kim *et al.* [16] have proposed a new concept to charge drones using electrification line (E-line). In their proposed approach, the batteries connected along the E-lines use a renewable energy source to store and produce the electricity. The stored electricity is wirelessly transmitted to a drone's battery through E-lines' inverter device, coiled lines, and drone's rectifier device consecutively

(see Figure 11 in Appendix A). The focus of their work was to extend the flight duration so that a drone can cover a longer borderline segment per each trip. This paper further extends their work to provide a method of continuous border surveillance without having to return frequently to their depots. Continuous monitoring sends live information about different locations of the borderline to the designated control centers, thus helping enhance border security and reduce the necessity of man-operated systems. Hence, we provide a method to determine the number of drones to cover the selected borderline and assign each drone to a segment of the borderline for the continuous surveillance. Some new features include the consideration of surveillance priority for different locations along the border, variable drone speed over the E-line when it is needed to gain more power to charge the drone battery from the E-line. Some locations may have a higher probability of being penetrated and are more critical than others. The proposed model provides more frequent surveillance to these critical locations to account for heterogeneous risk levels.

To find the optimal solution to this problem, we develop a multi-objective mixed-integer nonlinear programming (MINLP) model to find the optimal length and location of the E-line as well as the minimum required number of drones to be utilized. We also determine the drone flight path and its speed while passing the E-line. To solve the model, we develop two algorithms. The first algorithm determines Pareto-optimal solutions among all feasible solutions as a tool for decision-makers to identify the best solution suited to their investment preferences and budgetary constraints. The second algorithm provides an initial solution to the optimization model in order to expedite the computational process.

The rest of the paper is organized as follows. Section 2 explains the problem description, assumptions that are required for developing the optimization model, and the problem formulation. Section 3 presents the solution approach, including the propositions and algorithms that we implemented to solve the model and improve the problem-solving efficiency. In Section 4, we illustrate the methodology through a case study and numerical analysis. A sensitivity analysis is provided to examine and elaborate on the model behavior under different assumptions and parameters. Additionally, a cost analysis is performed to provide more insight to the decision-makers. Finally, Section 5 concludes the paper and suggests potential future research.

2. Problem Description and Formulation

To enhance the security of the nation's border, we propose a continuous flight of small drones over its perimeter. The battery limitation of a drone proves to be one of the main obstacles to a continuous flight time. In most cases, the battery duration of a small-size drone does not exceed 30 minutes. To address this problem, we propose to use the E-line system [16], which can charge the drones wirelessly. The E-line system with an appropriate length will charge the drones during their surveillance, enable a continuous and seamless flight over the border, and eliminate the need for battery charging depots. This work provides an optimization model to determine the optimal number of drones, the optimal length of the E-line, and the optimal location of the E-line system required for border surveillance. The optimization model will minimize the total length of the E-line system as well as the total number of drones for the operation. To enhance the awareness of the system and the security of the border, providing frequent flights to every location on the border is essential. Locations having a higher chance of being penetrated by intruders should hold a higher

priority and should be monitored more frequently. This is handled in our proposed optimization model by introducing the concept of *revisiting gap*, which is defined as the time interval between two consecutive visits to a particular point of the border. We assume that every location on the border is assigned its priority level, which helps determine the frequency of visit to the location. Hence, a permitted revisiting gap can be interpreted as the time interval a drone can be away from a particular location during the surveillance operation, and it is given to the optimization model as an input parameter.

Borders form continuous lines and may not have physical waypoints or breakpoints at every location. Hence, we assume equally-spaced waypoints distributed over the borderline for the convenience of developing an mathematical model. As the drone can fly over any objects on the ground, these points serve as virtual locations for the user to be able to control flight segments and the frequency of visits by drones. Having many (virtual) waypoints over the borderline (i.e., a higher resolution) can improve the accuracy of the model. But, it comes at the cost of a higher computational complexity for solving the optimization model. This is because, as the resolution increases, the corresponding number of variables in the optimization model increases significantly. Thus, we aim to find a sufficient number of waypoints to have a reasonable trade-off between the model accuracy and the computational complexity.

The following assumptions are made to develop the optimization model:

- The borderline will be divided into multiple border segments, and a drone will be assigned to each segment. This action assists in controlling the drones as well as avoiding the chances that more than one drone will visit any one location and collision among the drones [2].
- Each location on the border has a pre-assigned revisiting gap. This gap may differ based on the location. The locations with higher priority are assigned a shorter revisiting gap in order to enhance security.
- The battery discharging rate is constant, but the charging efficiency is a function of the drone speed.

In addition to the above assumptions, we suggest two different speeds during their flights: the nominal speed for normal operation and the charging mode speed for flying while being charged (i.e., flying above the E-line). To lessen the revisiting gap, drones should use their nominal speed while passing segments not covered by the E-line; however, they may reduce the speed when flying over the E-line to have more time to recharge their battery.

This problem involves several variables to be determined using an optimization model, which includes a sufficient number of drones, the total length of the E-line system, the speed of the drones, and the scanning pattern of each drone. However, the resulting mathematical model will be a complex non-convex model that may not be practical for solving the problem presented in this paper. Note that finding optimal scanning patterns for all drones alone is a combinatorial optimization problem, which is often difficult to solve. Therefore, we propose a two-phase sequential optimization approach. The first phase focuses on finding the optimal scanning pattern of each drone, and the second phase is to determine the remaining variables for the given scanning patterns.

2.1. Phase I: Scanning Pattern Determination

Since the borderline is divided into multiple border segments and a drone is assigned to each segment, each drone's flight range is limited to between the two endpoints (E_1 and E_2) of its segment (see Figure 1). Consider waypoint i located between E_1 and E_2. Let λ_i denote the distance between waypoint i and E_1, and μ_i be the distance between waypoint i and E_2. Each segment consists of several waypoints, and each of the way points may be associated with a different priority in terms of the risk level for penetration. There can be numerous scanning patterns for a drone surveillance for the segment, especially, when there are multiple waypoints and the priority level (i.e., risk) of each waypoint differs from each other. We define a *scanning pattern* of a drone as a routine sequence of drone flights that leaves a starting point, scan the segment, and return back to the starting point to complete one flight cycle, which will be repeated by the drone during the assigned surveillance operation period. Some example scanning patterns include $p_1 :=< i - E_2 - i - E_2 - E_1 - i >, p_2 :=< E_2 - i - E_2 - i - E_1 - i - E_2 >$, and $p_3 :=< i - E_2 - i - E_1 - i >$. Patterns p_1 and p_2 can be appealing if the priority of waypoints between i and E_2 is higher than the priority for the right sub-segment between E_1 and i. Hence, a scanning pattern selection approach is proposed to choose one of the many possible scanning patterns, which results in the minimum revising gap for a drone to fly repeatedly following the pattern.

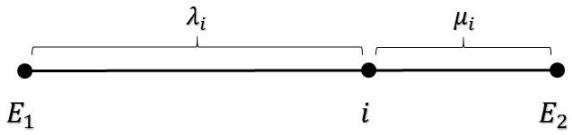

Figure 1: A segment of the borderline including waypoint i and its two endpoints, E_1 and E_2

We define $\mathcal{P}$ as the set of possible scanning patterns for the drone to scan a given area. In Figure 1, let t_{λ_i} be the flight time between waypoint i and E_1, and t_{μ_i} be the flight time between waypoint i and E_2. Following a fixed flight pattern p, the drone's revising gap to a specific waypoint i maybe different from one visit to the next. Our goal is to ensure that each waypoint is visited as frequently as possible, which can be accomplished by minimizing the maximum gap among all possible revisting gaps generated by a fixed scanning pattern. Let $\mathcal{G}_{i,k}(p)$ be the time interval between the k^{th} and $(k+1)^{st}$ visits of waypoint i following pattern $p \in \mathcal{P}$, a collection of all possible scanning patterns. Then, a maximum revisiting gap for waypoint i during the operation can be defined as $\mathcal{G}_i^{max}(p) = \max_{k\in\{1,2,\cdots,\bar{K}\}} \mathcal{G}_{i,k}(p)$.

Proposition 1 below shows that the minimum value of the maximum revisiting gap can be achieved if a drone flies between the two endpoints and changes its direction only at the endpoints. Let $\mathcal{G}_i^*$ be the minimum value of $\mathcal{G}_i^{max}$ over all patterns: $\mathcal{G}_i^* = \min_{p\in\mathcal{P}} \mathcal{G}_i^{max}(p)$. We have:

Proposition 1. *$\mathcal{G}_i^*$ for waypoint i during the surveillance operation is achieved if the drone flies directly and repeatedly between two endpoints E_1 and E_2, and $\mathcal{G}_i^* = 2 \cdot max(t_\lambda, t_\mu)$.*

Proof. See Appendix B. □

We use Proposition 1 to find optimal paths and eliminate the need for path planning in the optimization model, thus reducing the complexity of the model. For more efficient use of the E-line, we allow the drones to reduce their speed while flying over the E-line with the purpose of spending more time in charging mode. We also consider the charging efficiency from the E-line as a function of the drone's speed. Reducing the flight speed over the E-line facilitates control over the drone, reduces the drone's deviations from the E-line, and improves the charging efficiency [5]. The optimization model determines the optimal speed of the drones while they pass the E-line. However, to achieve a lower revisiting gap for the waypoints, the drones must fly at their maximum speed when they are not passing the E-line.

2.2. Phase II: Optimization Model Formulation

In this subsection, we first present the notation used in the model, and then provide the detailed formulation of the optimization model.

To illustrate the notation, Figure 2 shows an example of a segment of the borderline with its associated endpoints, a portion of the E-line (dotted line), and three waypoints $(i-1, i, i+1)$.

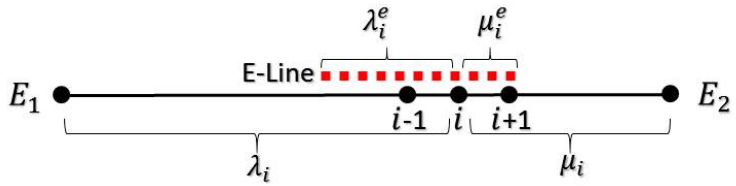

Figure 2: A segment of the borderline with its associated endpoints (E_1 and E_2) and a portion of the E-line (dotted line)

Variable λ_i represents the distance between waypoint i and E_1. If waypoint i is the first endpoint of a segment, it is also the second endpoint of the previous segment. Hence, λ_i would be equal to its distance from the first waypoint of the previous segment. Otherwise, λ_i is equal to the distance between its previous waypoint and E_1 plus its distance from the previous waypoint. The value of variable λ_i can be calculated using Equation (1).

$$\lambda_i = \begin{cases} \lambda_{i-1} + d, & if\ i \neq 0 \text{ and } p_{i-1} = 0 \\ d, & if\ i \neq 0 \text{ and } p_{i-1} = 1 \\ 0, & if\ i = 0 \end{cases} \tag{1}$$

Similarly, variable μ_i represents the distance between waypoint i and E_2. If waypoint i is the second endpoint of a segment, it is also the first endpoint of the next segment. So, μ_i would be equal to its distance from the second waypoint of the next segment. Otherwise, μ_i is equal to the distance between its next waypoint and E_2 plus its distance from the next waypoint. The value of

μ_i for each waypoint can be calculated as follows.

$$\mu_i = \begin{cases} \mu_{i+1} + d, & if\ i \neq n \text{ and } p_{i+1} = 0 \\ d, & if\ i \neq n \text{ and } p_{i+1} = 1 \\ 0, & if\ i = n \end{cases} \tag{2}$$

Variables λ_i^e and μ_i^e represent the distances between waypoint i and the two endpoints of the segment covered by the E-line. Equations (3) and (4) outline the calculation of the values λ_i^e and μ_i^e for each waypoint. The formulation is similar to Equations (1) and (2); in this case, the distance between two consecutive waypoints is replaced by the distance covered by the E-line between the same two waypoints. Variable e_i represents the distance between waypoints i and $i+1$ that is covered by the E-line.

$$\lambda_i^e = \begin{cases} \lambda_{i-1} + e_{i-1}, & if\ i \neq 0 \text{ and } p_{i-1} = 0 \\ e_{i-1}, & if\ i \neq 0 \text{ and } p_{i-1} = 1 \\ 0, & if\ i = 0 \end{cases} \tag{3}$$

$$\mu_i = \begin{cases} \lambda_{i+1} + e_i, & if\ i \neq n \text{ and } p_{i+1} = 0 \\ e_i, & if\ i \neq n \text{ and } p_{i+1} = 1 \\ 0, & if\ i = n \end{cases} \tag{4}$$

A multi-objective mixed-integer non-linear optimization model for obtaining the optimal solution is presented below. Equation (5.1) shows the objective functions of the model, and Equations (5.2) to (5.32) represent the constraints. The objective is to minimize the total number of drones (η) and the total length of the E-line system ($\mathcal{L}$).

$$Minimize \quad (\mathcal{L}, \eta) \tag{5.1}$$

Equation (5.2) ensures that the number of segments is equal to the number of drones. Equation (5.3) guarantees that the revisiting gap for waypoint i is less than or equal to the permitted revisiting gap. In Equation (5.3), the left hand side is variable and the right hand side is a parameter.

$$\sum_{i \in N} p_i = \eta \tag{5.2}$$

$$\delta_i \leq g_i, \qquad i \in N \tag{5.3}$$

Equations (5.4) to (5.8) calculate the distance between each waypoint and the first endpoint of its segment. Similarly, Equations (5.9) to (5.13) calculate the distance between each waypoint and the second endpoint of its segment. These equations are the linearized forms of Equations (1) and (2), respectively.

$$\lambda_i \leq \lambda_{i-1} + d, \qquad i \in N \setminus \{0\} \tag{5.4}$$
$$\lambda_i \leq M_1(1 - p_{i-1}) + d, \qquad i \in N \setminus \{0\} \tag{5.5}$$
$$\lambda_i \geq d, \qquad i \in N \setminus \{0\} \tag{5.6}$$
$$\lambda_i \geq \lambda_{i-1} + d - M_1 p_{i-1}, \qquad i \in N \setminus \{0\} \tag{5.7}$$
$$\lambda_0 = 0 \tag{5.8}$$
$$\mu_i \leq \mu_{i+1} + d, \qquad i \in N \setminus \{n\} \tag{5.9}$$
$$\mu_i \leq M_1(1 - p_{i+1}) + d, \qquad i \in N \setminus \{n\} \tag{5.10}$$
$$\mu_i \geq d, \qquad i \in N \setminus \{n\} \tag{5.11}$$
$$\mu_i \geq \mu_{i+1} + d - M_1 p_{i+1}, \qquad i \in N \setminus \{n\} \tag{5.12}$$
$$\mu_n = 0 \tag{5.13}$$

Equations (5.14) to (5.18) determine the portion of the borderline between the waypoint and the first endpoint of the segment that is covered by the E-line, and Equations (5.19) to (5.23) determine the portion of the line between a waypoint and the second endpoint of the segment that is covered by the E-line. Equations (5.14) to (5.18) and Equations (5.19) to (5.23) are the linearized forms of Equation (3) and (4), respectively.

$$\lambda_i^e \leq \lambda_{i-1}^e + e_{i-1}, \qquad i \in N \setminus \{0\} \tag{5.14}$$
$$\lambda_i^e \leq M_1(1 - p_{i-1}) + e_{i-1}, \qquad i \in N \setminus \{0\} \tag{5.15}$$
$$\lambda_i^e \geq e_{i-1}, \qquad i \in N \setminus \{0\} \tag{5.16}$$
$$\lambda_i^e \geq \lambda_{i-1}^e + e_{i-1} - M_1 p_{i-1}, \qquad i \in N \setminus \{0\} \tag{5.17}$$
$$\lambda_0^e = 0 \tag{5.18}$$
$$\mu_i^e \leq \mu_{i+1}^e + e_i, \qquad i \in N \setminus \{n\} \tag{5.19}$$
$$\mu_i^e \leq M_1(1 - p_{i+1}) + e_i, \qquad i \in N \setminus \{n\} \tag{5.20}$$
$$\mu_i^e \geq e_i, \qquad i \in N \setminus \{n\} \tag{5.21}$$
$$\mu_i^e \geq \mu_{i+1}^e + e_i - M_1 p_{i+1}, \qquad i \in N \setminus \{n\} \tag{5.22}$$
$$\mu_n^e = 0 \tag{5.23}$$

Equations (5.24) and (5.25) calculate the revisiting gap at each waypoint. Equation (5.24) calculates the total time that the drone needs to travel from each waypoint to the first endpoint of the segment and then to return. Likewise, Equation (5.25) obtains the total time needed for the drone to travel from each waypoint to the second endpoint of the segment and then to return.

$$\delta_i \geq 2(\frac{\lambda_i - \lambda_i^e}{V} + \frac{\lambda_i^e}{V^e}), \qquad i \in N \tag{5.24}$$

$$\delta_i \geq 2(\frac{\mu_i - \mu_i^e}{V} + \frac{\mu_i^e}{V^e}), \qquad i \in N \tag{5.25}$$

Equations (5.26) to (5.28) guarantee that the drone's battery is sufficiently charged at the time of operation. Equation (5.26) ensures that during a trip between the endpoints of a segment, the battery charge percentage that a drone gains by flying above the E-line is no less than the power required for that trip. Equations (5.27) to (5.28) are set to ensure that at each waypoint, the drone has enough battery to fly to an endpoint and to return.

$$\theta_{dis}\frac{\mu_i - \mu_i^e}{V} \leq \theta_{ch}\frac{\mu_i^e}{V^e}\phi_e - \theta_{dis}\frac{\mu_i^e}{V^e} + M_2(1 - p_i), \qquad i \in N \tag{5.26}$$

$$2(\theta_{dis}\frac{\mu_i - \mu_i^e}{V} - \theta_{ch}\frac{\mu_i^e}{V^e}\phi_e) \leq 100 - \varepsilon, \qquad i \in N \tag{5.27}$$

$$2(\theta_{dis}\frac{\lambda_i - \lambda_i^e}{V} - \theta_{ch}\frac{\lambda_i^e}{V^e}\phi_e) \leq 100 - \varepsilon, \qquad i \in N \setminus 0 \tag{5.28}$$

Equation (5.29) ensures that the total length of the E-line is the summation of the length of the E-line between each two consecutive segments. Equation (5.30) enforces that the length of the E-line between every two waypoints cannot exceed the distance between them. Equation (5.31) limits the first waypoint to being the first endpoint of a segment, and Equation (5.32) controls the range of the variables.

$$\mathcal{L} = \sum_i e_i, \qquad i \in N \tag{5.29}$$

$$e_i \leq d, \qquad i \in N \tag{5.30}$$

$$p_0 = 1, \tag{5.31}$$

$$e_i, \delta_i, \lambda_i, \mu_i, \lambda_i^e, \mu_i^e \geq 0 \qquad i \in N \tag{5.32}$$

3. Solution Approach

In this section, we describe the proposed approaches used to solve the optimization model. We first note that the problem contains multiple objectives; there is a need for minimizing the total number of drones and the total length of the E-line. Approaches most commonly used to solve such problems are the Preemptive Goal Programming approach or creating a single objective by using a linear weighted objective function. However, for this model, prioritizing the objectives and discovering the optimal trade-off between the total length of the E-line and the total number

of drones is not a straightforward task. Additionally, since the operational cost estimates may not be accurate and because the useful life of the E-lines is not known in advance, it is not possible to simplify the objective function into the total cost. Hence, there is a need for an approach that provides the Pareto-optimal solutions. Equations (5.24) to (5.28) are also non-linear and may result in a longer computational time to solve the model [22]. To address these two issues, we propose solving the model in multiple iterations. In each iteration, we fix the E-line passing speed (V^e) and solve the model for that specific speed. Next, we find the optimal set for the E-line passing speed in the next level. Proposition 2 states that fixing the E-line passing speed helps to facilitate the process of finding a proper trade-off between the E-line length and the number of drones:

Proposition 2. *If the speed of the drones flying above the E-line is fixed, the optimal length of the E-line is also fixed, and equals:*

$$\mathcal{L} = \frac{V^e \theta_{dis} \mu_i}{\phi_e V \theta_{ch} + V^e \theta_{dis} - V \theta_{dis}} D \tag{6}$$

Proof. To calculate the total length of the E-line system, first we calculate the E-line length in each segment. From Equation (5.26), for each waypoint i, we have:

$$\begin{aligned}
&\theta_{dis}\frac{\mu_i - \mu_i^e}{V} \leq \theta_{ch}\frac{\mu_i^e}{V^e}\phi_e - \theta_{dis}\frac{\mu_i^e}{V^e} + M(1-p_i) \\
\Longrightarrow &\theta_{dis}\frac{\mu_i}{V} \leq \theta_{dis}\frac{\mu_i^e}{V} + \theta_{ch}\frac{\mu_i^e}{V^e}\phi_e - \theta_{dis}\frac{\mu_i^e}{V^e} + M(1-p_i) \\
\Longrightarrow &\theta_{dis}\frac{\mu_i}{V} \leq \mu_i^e\left(\frac{\theta_{dis}}{V} + \frac{\theta_{ch}}{V^e}\phi_e - \frac{\theta_{dis}}{V^e}\right) + M(1-p_i) \\
\Longrightarrow &\mu_i^e \geq \frac{V^e \theta_{dis}\mu_i - M(1-p_i)VV^e}{\phi_e V \theta_{ch} + V^e \theta_{dis} - V\theta_{dis}}
\end{aligned} \tag{7}$$

Suppose that waypoint i is the first endpoint of segment k, (i.e. $p_i = 1$). Then, the length of the E-line in segment k equals μ_i^e. Thus,

$$E_k = \mu_i^e \geq \frac{V^e \theta_{dis}\mu_i}{\phi_e V \theta_{ch} + V^e \theta_{dis} - V\theta_{dis}}. \tag{8}$$

The total length of E-line ($\mathcal{L}$) is the summation of E_k for all segment. Hence,

$$\mathcal{L} = \sum_k E_k = \sum_{i|p_i=1} \mu_i^e \geq \sum_{i|p_i=1} \frac{V^e \theta_{dis}\mu_i}{\phi_e V \theta_{ch} + V^e \theta_{dis} - V\theta_{dis}}. \tag{9}$$

Also,

$$\begin{aligned}
\sum_{i|p_i=1} \frac{V^e \theta_{dis}\mu_i}{\phi_e V \theta_{ch} + V^e \theta_{dis} - V\theta_{dis}} &= \frac{V^e \theta_{dis}}{\phi_e V \theta_{ch} + V^e \theta_{dis} - V\theta_{dis}} \sum_{i|p_i=1} \mu_i \\
&= \frac{V^e \theta_{dis}}{\phi_e V \theta_{ch} + V^e \theta_{dis} - V\theta_{dis}} D.
\end{aligned} \tag{10}$$

By using Equation (9) and Equation (10), we have:

$$\mathcal{L} \geq \frac{V^e \theta_{dis}}{\phi_e V \theta_{ch} + V^e \theta_{dis} - V \theta_{dis}} D. \tag{11}$$

In Equation (11), if V^e is known, the right-hand side is a fixed parameter. Since the model attempts to minimize the total length of the E-line and the E-line length is a continuous variable, the equality in Equation (8) holds, which is the total length of the E-line. □

From Proposition 2, we conclude that by fixing the speed of the drones over the E-line, the two goals in the objective function become independent of one another in each iteration. Instead of finding an optimum trade-off between the number of drones and the total length of the E-line, we can minimize both terms simultaneously. Thus, the length of the E-line is removed from the objective function and is fixed as Equation (11). An accurate prediction of the total cost of both the E-line and the drones is not easy to obtain, as the costs may vary from time to time. This replacement helps decision-makers analyze cost in the post-optimization stage and find an appropriate trade-off between the number of drones and the total length of the E-line. Also, constraints (5.24) to (5.28) have a variable as the denominator and are non-convex. Fixing the speed of the drones while they pass the E-line reconstructs the denominators into parameters and converts these equations into convex equations. In each iteration, the value of the E-line passing speed is given to the optimization model, and changing the value of this parameter may result in attaining different optimal solutions. Hence, to obtain the optimal solution to the problem, the value of this parameter needs to be determined.

Flying at a lower speed over the E-line will result in a higher revisiting gap for each waypoint. In other words, if a drone flies at a lower speed, there is a need for more drones to meet the permitted revisiting gap. This makes the required number of drones needed to satisfy the revisiting gap constraint a non-increasing function of the E-line passing speed. Inversely, the total optimal length of the E-line is an increasing function of the E-line passing speed (see Proposition 3 in Appendix C).

The objective of the model is to minimize both the number of drones and the total length of the E-line. Since the number of drones is a decreasing step function and the total length of the E-line is an increasing function, the Pareto-optimal solutions occur at the E-line passing speed where the required number of drones drop. We call V^e a *critical speed* if it provides a Pareto-optimal solution. At this speed, the required number of drones is less than the corresponding number of drones needed for the E-line passing speed of $V^e - \varepsilon_V$, where ε_V is an arbitrarily chosen parameter for the accuracy of the model. If the model confirms V^e as a critical speed, the actual critical speed has a value within $[V^e - \varepsilon_V, V^e + \varepsilon_V]$. To illustrate this, suppose that Figure 3 showcases the optimal number of drones (η^*) and the length of the E-line for different values of the E-line passing speed. In this problem, 1 mph, 5 mph, and 25.7 mph are chosen as the critical speeds, thus providing three possible optimal solutions for the decision-makers to choose from considering the investment and budgetary constraints.

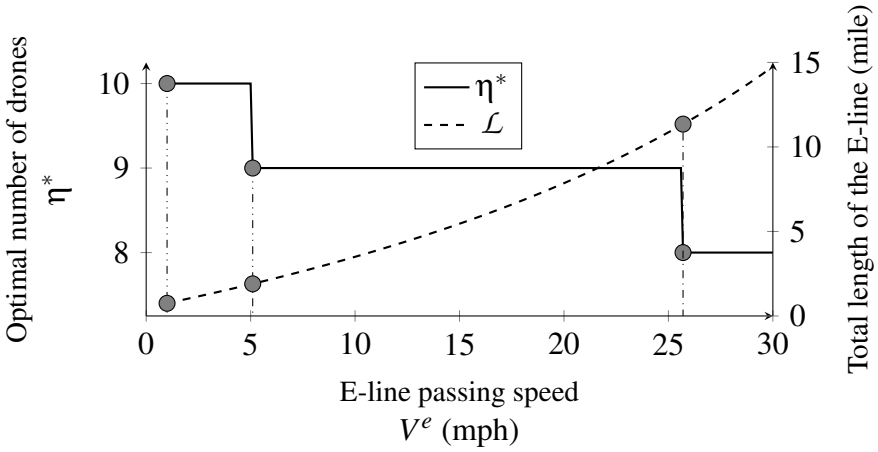

Figure 3: An Example of Optimal Number of Drones and Length of the E-line

Algorithm 1 has been developed to find the critical speeds within in a short computational time. The result can assist in finding a set of candidate optimal solutions to the problem.

Algorithm 1 Finding Critical Speeds

Inputs:

ε_V : The accuracy of finding the critical speeds

function $\eta^*(V^e)$

Fix $\mathcal{L} = \frac{V^e\theta_{dis}}{\phi_e V\theta_{ch}+V^e\theta_{dis}-V\theta_{dis}}D$

Solve the model (5) with the objective function $\eta^*_{V^e}$= Min η and Constraints (5.2) to (5.32)

Return the optimal objective value

end function

function FINDCRITICAL(V^e_{min}, V^e_{max})

if $\eta^*_{V^e_{min}} = \eta^*_{V^e_{max}}$ **then**

$\forall V^e \in [V^e_{min}, V^e_{max}]$ set $\eta^*_{V^e} = \eta^*_{V^e_{min}}$

else if $V^e_{max} - V^e_{min} > \varepsilon$ **then**

$V^e = \frac{V^e_{min}+V^e_{max}}{2}$

Round V^e by ε_V

Use $\eta^*_{V^e_{min}}$ and $\eta^*_{V^e_{max}}$ as the upper and lower bound of the objective function, respectively.

Find $\eta^*(V^e)$

FINDCRITICAL(V^e_{min}, V^e)

FINDCRITICAL(V^e, V^e_{max})

end if

end function

Procedure:

V^e_{min} = minimum possible speed for the drone (e.g., 1 mph)

V^e_{max} = maximum speed for the drone (e.g., 30 mph)

Find $\eta^*(V^e_{min})$

Find $\eta^*(V^e_{max})$

FINDCRITICAL($\eta^*(V^e_{min}), \eta^*(V^e_{max})$)

for all V^e if $\eta^*_{V^e} < \eta^*_{V^e-\varepsilon_V}$, V^e is a critical speed.

In Algorithm 1, the optimization model (5) is solved for every value of the E-line passing speed. The proposed model is a mixed-integer linear optimization problem with both equality and inequality constraints. Thus, solving the model for each value of V^e can be time-consuming. Table 1 shows the correlation between the problem size and the number of waypoints.

Table 1: Size of the problem with n waypoints

Number of waypoints (n)	20	50	100	150	200
Number of variables	138	348	698	1048	1398
Number of constraints	427	1087	2187	3287	4387

Using a warm start solution is an effective strategy to reduce the computation time of the model [23]. Hence, Algorithm 2 is developed to help solving the optimization model. The solution output by Algorithm 2 provides a good initial solution to the exact model. In this algorithm, $\mathcal{V}$ stands for the set of candidate values for the E-line passing speed; $\mathcal{E}^1_i$ and $\mathcal{E}^2_i$ indicate the first and second

endpoints of the segment in which waypoint i is located, respectively; l is the portion of each area that is covered by the E-line using Equation (11); R_i is the furthest distance that the drone can fly from waypoint i; f_i equals 1 if the solution is feasible based on the gap constraint related to waypoint i and 0 otherwise; and c is the counter for the last infeasible waypoint. This algorithm simplifies the problem by considering that the distance between all neighboring waypoints is covered by some constant length of the E-line. The length of the E-line between two neighboring waypoints is calculated by Equation (11). This allows for a decreased model size, as the model is no longer required to make any decisions about E-line location. The solution provided by Algorithm 2 can be solved in less than a second and is used as an initial solution to the exact model.The performance of this algorithm is discussed in the numerical experiment section.

Algorithm 2 Heuristic Algorithm to Provide Initial Solution

for $V^e \in \mathcal{V}$ **do**
  $p_1 = 0$, $\mathcal{E}_1^1 = 1$, $\mathcal{E}_n^2 = n$
  $l = \frac{V^e \theta_{dis}}{\phi_e V \theta_{ch} + V^e \theta_{dis} - V \theta_{dis}}$
  $R_i = g_i \frac{\varphi_{V^e} V \theta_{ch} + V^e \theta_{dis} - V \theta_{dis}}{2 \varphi_{V^e} \theta_{ch}} d$
  do
    $c = 0$
    for i = 2 to n **do**
      $f_i = 1$
      $\delta_i = \min_{\mathcal{E}_i^2 \le j \le i} \frac{r_j}{d+j}$
      if $p_{i-1} = 1$ **then**
        $\mathcal{E}_i^1 = i - 1$
      else
        $\mathcal{E}_i^1 = \mathcal{E}_{i-1}^1$
      end if
      if $d(i - \mathcal{E}_i^1) > R_i$ or $i > \delta_i$ **then**
        $f_i = 0$
        $c = i$
      end if
    end for
    if $c > 0$ **then**
      if $p_{c-1} = 1$ **then**
        The problem does not have a feasible solution.
      else
        $p_{c-1} = 1$
      end if
    end if
  while $c > 0$
  $\eta_{V^e} = \sum_{\forall i \in N} p_i$
  $\mathcal{L} = \frac{V^e \theta_{dis}}{\phi_e V \theta_{ch} + V^e \theta_{dis} - V \theta_{dis}} D$
end for

4. Numerical Experiments

This section details a case study and the numerical results of the proposed model (5). A sensitivity analysis is performed in Section 4.3 to understand the model behavior considering the different number of waypoints and side goals associated with this model.

4.1. Case Study

A segment of the U.S.-Mexico borderline spanning 22.8 miles and located between two border crossings is considered for the case study in this section. This borderline is located within the Cochise County limits in Arizona (Figure 4). The west side of the borderline is located at the border crossing in Naco, Arizona (Point A), and the east side is located at the crossing in Douglas, Arizona (Point B).

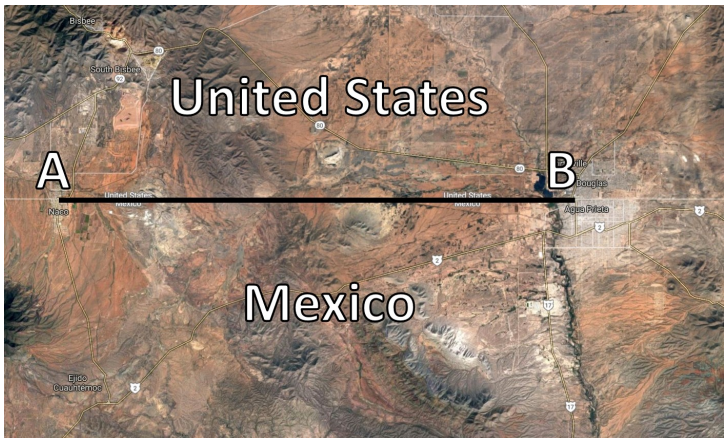

Figure 4: Case Study, US - Mexico Border

Figure 5 shows the randomly generated permitted revisiting gap for every location of this borderline. The time allotted for each given revisiting gap at each location varies between a range of 5 to 20 minutes, and this given time is based on the risk of penetration. The locations detailing higher risk need more frequent surveillance and have a shorter given revisiting gap. Table 2 presents the rest of the parameters. By considering $n = 200$, the borderline is divided into two hundred sub-sections with 201 equally distributed waypoints. The maximum charging rate is assumed to be 10% per minute, and the discharging rate is set to 2.5% per minute. This entails that the drone can fly up to 40 minutes without charging and that it can fully recharge by flying for roughly 13 minutes over the E-line.

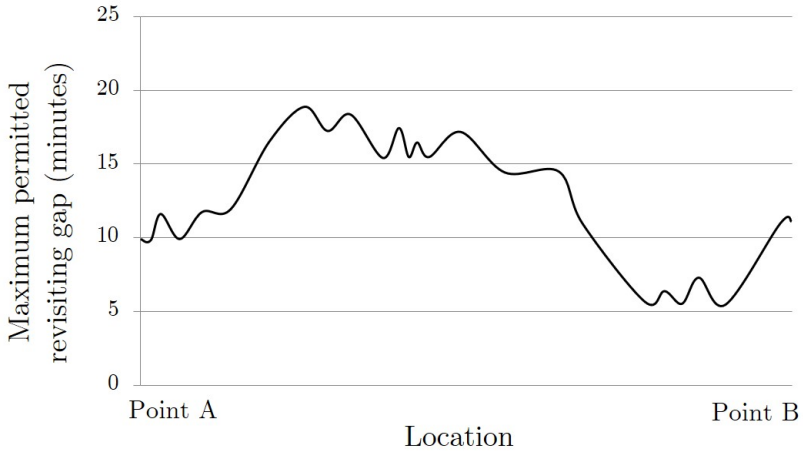

Figure 5: Maximum permitted revisiting gap for each location

Table 2: Parameters used as inputs of the case study

θ_{dis}	Discharging rate	2.5% per min
θ_{ch}	Nominal charging rate for flying over the E-line	10% per min
V	Maximum drone speed	30 mph
ε	Minimum allowed battery charge	5%
ϕ_e	Charging efficiency function	$1-\frac{V^e}{100}$
D	Total length of border covered (mile)	22.8 miles
N	Set of waypoints	{0,...,200}
d	Distance between two consecutive waypoint	0.114 mile

4.2. Numerical Results

The case study results is generated by implementing Algorithm 2. In other words, Algorithm 2 provides an initial solution and consequently helps to solve the proposed optimization model (5). Algorithm 1 is implemented to find the candidate optimal solutions to the problem. The speed margin for the critical speed is set to 0.1 mph (i.e., $\varepsilon_V = 0.1$), meaning that the actual critical speeds are within 0.1 mph from our findings. The minimum and maximum speeds for the drone are set to 1 mph and 30 mph, respectively. Figure 6 depicts the effect of different quantities of V^e on the optimal number of drones (η) and the total length of the E-line ($\mathcal{L}$). The range of the required number of drones falls between 10 and 14 for various values of the E-line passing speeds. The numerical results show that five candidate solutions exist for this problem.

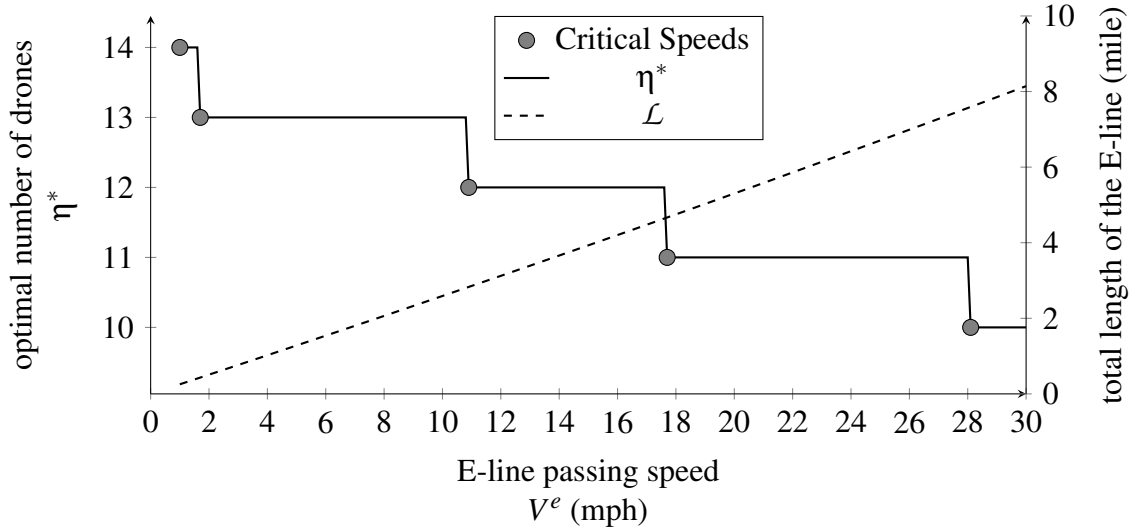

Figure 6: Optimal Number of Drones and Length of the E-line

Table 3 shows the candidate solutions that the decision-makers can consider to achieve an optimal solution.

Table 3: Candidate Solutions for the Case Study

	CS_{1^*}	CS_2	CS_3	CS_4	CS_5
Speed (V^e)	1	1.7	10.9	17.7	28.1
Number of Drones (η)	14	13	12	11	10
Total Length of the E-line ($\mathcal{L}$)	0.254	0.432	2.830	4.668	7.593

*$CS_{\#}$ = Candidate Solution #

To obtain a better understanding of the results, let us arbitrarily choose an E-line passing speed of 10.9 mph (i.e., $V^e = 10.9$). As shown in column CS_3 in Table 3, this speed is considered a critical speed. The optimal number of drones and the optimal length of the E-line are 12 and 2.83 miles, respectively. The segments corresponding to each drone and the locations of the installed E-line are presented in Table 4 and Table 5, respectively. Drones are assigned to border segments with different lengths. For instance, Drone 3 is designated to cover waypoints 39 to 67 with a length of 3.192 miles and has an average given revisiting gap of 18.41 minutes. Drone 9 is designated to cover a segment spanning 1.026 miles and has a permitted revisiting gap of 5.4 minutes. This demonstrates that the segments that have waypoints with shorter given revisiting gaps are shorter than the segments with longer given revisiting gaps (Table 4).

Table 4: Border Segment Assigned to Each Drone for CS_3

Drone ID	Assigned Waypoints	Covered Length (Miles)	E-line Length (Miles)	Average Permitted Revisiting Gap
1	0 to 18	2.052	0.254	10.79
2	18 to 39	2.394	0.297	13.36
3	39 to 67	3.192	0.396	18.41
4	67 to 94	3.078	0.382	16.82
5	94 to 121	3.078	0.382	16.29
6	121 to 139	2.052	0.254	13.42
7	139 to 151	1.368	0.17	8.46
8	151 to 160	1.026	0.127	5.70
9	160 to 169	1.026	0.127	5.40
10	169 to 178	1.026	0.127	6.40
11	178 to 188	1.14	0.142	5.73
12	188 to 200	1.368	0.17	8.92

Table 5: Location of the E-line in CS_3

Related Drone(s)	Location (Waypoints)	Length (Miles)
1	0 to 2	0.127
1 and 2	16 to 19	0.308
2 and 3	37 to 40	0.314
3 and 4	65 to 69	0.356
4 and 5	92 to 96	0.382
5 and 6	119 to 123	0.351
6 and 7	137 to 140	0.212
7 and 8	150 to 152	0.116
8 and 9	159 to 161	0.192
9 and 10	168 to 170	0.127
10 and 11	177 to 179	0.102
11 and 12	187 to 189	0.156
12	199 to 200	0.085

4.3. Sensitivity Analysis

This section analyzes the model behavior by changing some parameter values as well as the objective function of the model.

4.3.1. Number of Waypoints and Model Performance

In this study, we have assumed that each location at the borderline has a given revisiting gap. However, the model considers given revisiting gaps only for waypoints. Thus, increasing the number of waypoints may enhance the accuracy of the model and allow for the assignment of drones to more specific areas. However, having a higher number of waypoints makes it computationally more difficult to solve the model due to the increase in problem size (see Table 1). The case study was used to compare the CPU times for solving the model with and without using Algorithm 2. Figure 7 shows the improvement in the speed of the model for solving the problem after using the heuristic algorithm.

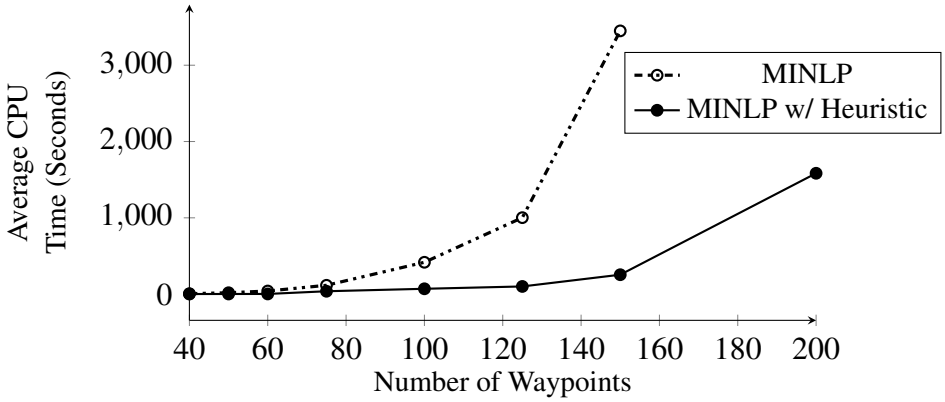

Figure 7: Comparing the computational time with and without using the heuristic algorithm

It is observed in Figure 7 that solving the cases that included more waypoints resulted in higher CPU times. However, implementing Algorithm 2 significantly reduced the CPU time. For example, it took approximately an hour to solve the situation involving 150 waypoints when the heuristic algorithm was not used. When the heuristic algorithm was utilized, however, CPU time was reduced by 92.6% (i.e., 254 seconds). Additionally, the model could not be solved in less than an hour for instances with more than 150 waypoints if no heuristic algorithm was used.

A higher number of waypoints elevates the CPU time necessary for solving the model. However, it provides higher resolution information on the risk associated with each border location. It also provides more options for assigning drone surveillance location. Figure 8 compares the performance of the model using 50, 100, and 200 waypoints on the border. The comparison indicates that by using a higher number of waypoints, the model is able to reach a solution with fewer drones for each V^e.

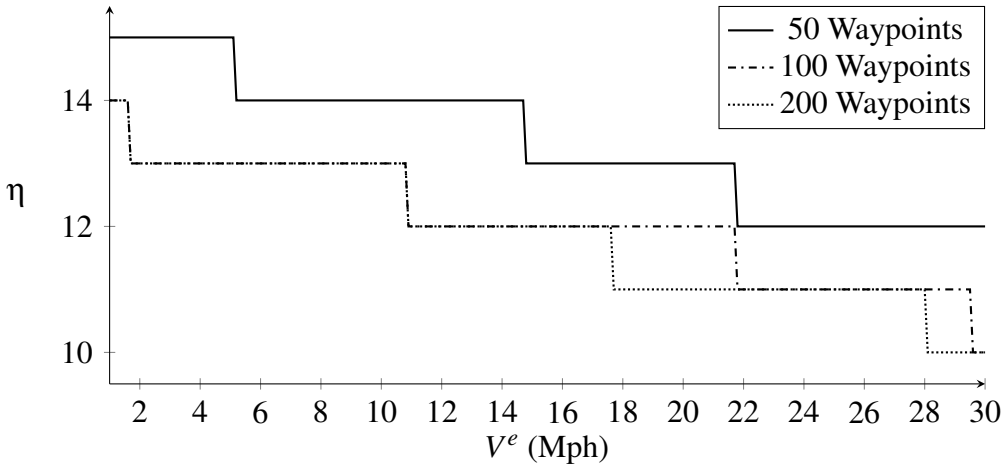

Figure 8: Sensitivity Analysis on changing the number of waypoints

4.3.2. Multiple Objectives

As discussed in Section 3, by fixing the E-line passing speed, the length of the E-line can be eliminated from the objective function. This changes the objective function by including only the number of drones. Results are also affected in the sense that a broad range of optimal solutions are now found. Thus, another term can be included in the objective function as a side goal. In Equation (12), the summation of the revisiting gaps of all waypoints is added to the objective function in order to find a low-risk solution. Nonetheless, this side goal is replaceable by other terms based on the preference of the decision-makers. For instance, one may prefer maximizing the safety margin, which is defined as the minimum difference between the given revisiting gap and the actual revisiting gap among all waypoints (i.e., $\gamma = min(g_i - \delta_i)$. To this aim, the objective function can be replaced by Equation (13), and Constraint (14) can be added to the model in Formulation (5).

$$\text{Model 1} : \textit{Minimize } M\eta + \sum_{i \in N} \delta_i \tag{12}$$

$$\text{Model 2} : \textit{Minimize } M\eta - \gamma \tag{13}$$

$$\gamma \leq g_i - \delta_i \qquad i \in N \tag{14}$$

Let us consider two cases in which two distinct side goals are examined: 1) Model 1, with intents to minimize the summation of the revisiting gaps for all nodes, and 2) Model 2, with intents to maximize the safety margin. Table 6 compares the solutions for these two cases. Model 1 obtained a solution with an average of 7.10 minutes for the revisiting gap at each waypoint, while the Model 2 solution had an average of 7.93 minutes for each waypoint. Furthermore, the safety margin determined by Model 2 is about 4 seconds (31%) higher than the solution of Model 1. Changing the side goal affects the segments allocated to each drone as well as the location of the E-line. However, the total E-line length and the number of drones remain the same.

Table 6: Sensitivity analysis on considering a side goal

	Model 1	Model 2
Total revisiting gap (Min)	1419.86	1585.27
Average revisiting gap (Min)	7.10	7.93
Safety margin (Sec)	12.36	16.20

Alternatively, other combinations of safety margin and revisiting gap goals can be explored based on the decision-makers' priorities to control both of them.

4.4. Cost Analysis

The optimization model presented in Section 2 determines a set of candidate solutions for the decision-makers. We suggest a method to help select an optimal solution among the candidate solutions. To find a proper trade-off between the length of the E-line and the number of drones, one approach can be to consider the total cost associated with the E-line and the drones. The total cost of the proposed approach can be divided into three groups: 1) installation cost of the E-line, 2) acquisition cost of the drones, and 3) operations and maintenance cost of the drones. Assume that there are two different types of drones. We take into account the yearly operation cost of each drone. The installation cost of the E-line and the acquisition cost of each drone are taken into account at the beginning of the program and after their useful life. Equation (15) calculates the total cost.

$$\begin{aligned} \text{Total Cost } &= \text{Operation Cost + E-line Installation Cost + Drone Acquisition Cost} \\ &= C_O\eta + C_I\mathcal{L} \times (A/P, i\%, N_E) + C_D\eta \times (A/P, i\%, N_D) \end{aligned} \tag{15}$$

In Equation (15), C_O is the operation cost per drone per year; C_I is the E-line installation cost per each mile; i is the yearly interest rate; N_E and N_D are the useful life of the E-line and the drones, respectively; and C_D is the acquisition cost of each drone.

Let us assume that: (i) drone Type I has a maximum flight time of 40 minutes and a maximum speed of 30 mph; (ii) drone Type II has a maximum flight time of 30 minutes and a maximum speed of 40 mph; and (iii) the minimum E-line passing speed is 5 mph. Table 7 presents the candidate solutions for both drone Type I and drone Type II, and Figure 9 compares the optimal number of drones and the total length of the E-line for each drone type.

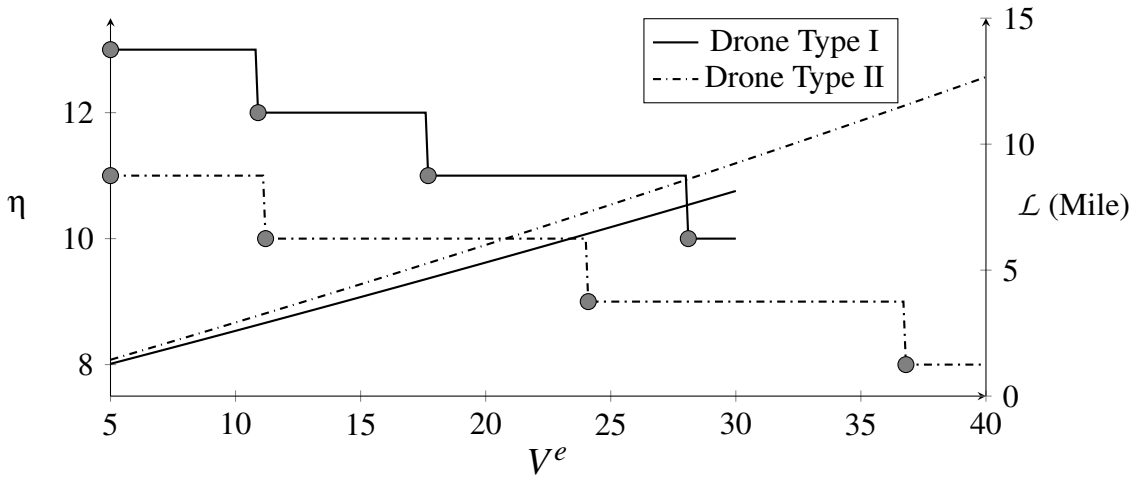

Figure 9: Optimal Number of Drones and Optimal Length of the E-line for Different Drone Types

Table 7: Candidate Solutions for Drone Type I and II

	Drone Type I				Drone Type II			
	CS_{1^*}	CS_2	CS_3	CS_4	CS_5	CS_6	CS_7	CS_8
Speed (V^e)	5	10.9	17.7	28.1	5	11.2	24.1	36.8
Number of Drones (η)	13	12	11	10	11	10	9	8
Total Length of the E-line ($\mathcal{L}$)	1.28	2.83	4.67	7.59	1.44	3.28	7.31	11.55

*$CS_{\#}$ = Candidate Solution #

Figure 9 illustrates that, when assigned to the same E-line passing speed, Type II drones need more utilization of the E-line than Type I drones. This is because Type II drones have a shorter flight time compared to Type I drones and needs more of the E-line for adequately charging its batteries. Furthermore, Type II drones have a higher maximum speed, which decreases the required number of drones needed to provide continuous surveillance.

Table 8 highlights the optimal decisions with the lowest total cost for different drone operation costs, and E-line installation cost. For instance, when the annual operation cost of each drone is \$100K and the installation cost of the E-line is \$400 per mile, the optimal solution suggests having 10 Type II drones and 3.28 miles of the E-line. It is observable that if the E-line price is much higher than drone costs, the optimal solution would suggest having more drones and a shorter length of the E-line. Contrarily, higher operation cost or increased drone acquisition cost results in an optimal solution suggesting fewer drones and more E-line.

Table 8: Cost Analysis

Inputs		Optimal Solution					
C_O ($K)	C_I ($K)	Candidate Solution	Total Cost ($K)	Drone Type	η	$\mathcal{L}$ (Miles)	V^e (Mph)
70	500	CS1	1,119	I	13	1.28	5.0
60	300	CS_3	948	I	11	4.67	17.7
80	200	CS_4	1,094	I	10	7.59	28.1
100	400	CS_6	1,414	II	10	3.28	11.2
100	200	CS_8	1,454	II	8	11.55	36.8

$i = 5\%$, $N_E = 10$ years, $N_D = 2$ years, $C_{D_I} = \$20$k, $C_{D_I} = \$50$k

Figure 10 presents the optimal solutions associated with the different drone operation costs and the E-line installation costs when the yearly interest rate is fixed at 5% (i.e., $i = 5\%$). The acquisition cost of Type I drone ($20K) is less than the acquisition cost of Type II drone($50K). However, the required number of Type II drones for the same length of the E-line is fewer than Type I drones. Hence, higher drone operation cost results in choosing Type II drones over Type I drones. Also, if the drone type is given, the optimal solution in a case of higher E-line installation cost is the candidate solution with the shortest length of the E-line and a greater amount of required drones (i.e., CS1 or CS_5). However, increasing the drone operation cost while fixing the E-line installation cost results in choosing the candidate solutions with fewer drones and more E-line (i.e., CS_4 and CS_8).

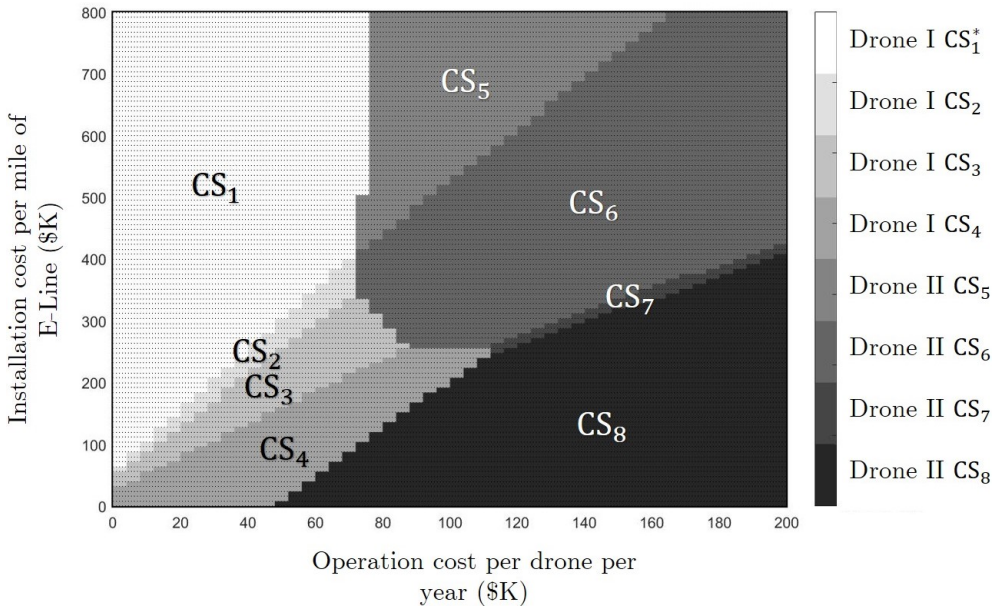

Figure 10: Optimal solution of the problem based on different values of C_O and C_I considering $i = 5\%$
*CS: Candidate solutions presented in Table 7

5. Conclusion

The U.S. has spent a significant amount of funds to secure its national borders. Border patrol requires many patrol agents who are assigned to different segments of the border. These patrol agents spend hours a day driving and hiking mostly uninhabited grasslands and mountain ranges, exposing them to dangerous environments. To enhance the security of the national borders and reduce the need for patrolling via human agents, this paper proposed the use of drones coupled with the use of E-lines for continuous border surveillance. Because different segments of the border exhibited different risk levels for invasion, this paper considered the risk associated with each location on the border to provide more frequent surveillance to higher-risk locations. We proved that the minimum time gap between two consecutive visits of each location is achieved if each drone flies directly between the two endpoints of its assigned segment. A multi-objective mixed-integer non-linear programming model was developed to find the optimal length and location of the E-line as well as the minimum required number of drones. Also, to gain more power from the E-line, we considered the option of having drones fly at lower speeds while passing the E-line. It was proved that fixing the drones' E-line passing speed allows the model to simultaneously minimize the number of drones and the total length of the E-line. Through this, we could eliminate the nonlinearity of the model and reduce the computation time and complexity. An algorithm was developed to find the candidate E-line passing speeds that provide Pareto-optimal solutions. Among these Pareto-optimal solutions given, the decision-makers can determine the optimal solution based on their financial strategies. Moreover, a heuristic algorithm was proposed to provide a proper initial solution for the model in order to accelerate the solving procedure. In the numerical example section, a case study of the U.S.-Mexico border was used to illustrate the model performance. The numerical results stated that continuous surveilling of the borderline could be realized by the implementation of the drones and the E-line. A sensitivity analysis was performed to examine and elaborate on the model behavior under different scenarios. Additionally, a cost analysis was provided to facilitate the decision-making process. For future work, one can consider both the dynamic and static charging stations for the drones over the border and the dynamic risk associated with different locations.

References

[1] Abushahma, Rema Ibrahim Hamad and Ali, Musab AM and Rahman, Nur Adilah Abd and Al-Sanjary, Omar Ismael. Comparative Features of Unmanned Aerial Vehicle (UAV) for Border Protection of Libya: A Review. In *2019 IEEE 15th International Colloquium on Signal Processing & Its Applications (CSPA)*, pages 114–119. IEEE, 2019.

[2] Ahmadian, Navid and Lim, Gino J and Torabbeigi, Maryam and Kim, Seon Jin. Collision-Free Multi-UAV Flight Scheduling for Power Network Damage Assessment. In *2019 International Conference on Unmanned Aircraft Systems (ICUAS)*, pages 794–798. IEEE, 2019.

[3] Bevacqua, Giuseppe and Cacace, Jonathan and Finzi, Alberto and Lippiello, Vincenzo. Mixed-initiative planning and execution for multiple drones in search and rescue missions. In *Twenty-Fifth International Conference on Automated Planning and Scheduling*, 2015.

[4] Bhatt, Manish R. Solar power unmanned aerial vehicle: High altitude long endurance applications (HALE-SPUAV). *A project presented to The Faculty of the Department of Mechanical and Aerospace Engineering, San Jose State University*, 2012.

[5] Bi, Zicheng and Kan, Tianze and Mi, Chunting Chris and Zhang, Yiming and Zhao, Zhengming and Keoleian, Gregory A. A review of wireless power transfer for electric vehicles: Prospects to enhance sustainable mobility. *Applied Energy*, 179:413–425, 2016.

[6] Bier, David J and Feeney, Matthew. *Drones on the Border: Efficacy and Privacy Implications*. Cato Institute, 2018.

[7] Bolkcom, Christopher and Nuñez-Neto, Blas. Homeland security: Unmanned aerial vehicles and border surveillance. LIBRARY OF CONGRESS WASHINGTON DC CONGRESSIONAL RESEARCH SERVICE, 2008.

[8] Dorling, Kevin and Heinrichs, Jordan and Messier, Geoffrey G and Magierowski, Sebastian. Vehicle routing problems for drone delivery. *IEEE Transactions on Systems, Man, and Cybernetics: Systems*, 47(1):70–85, 2017.

[9] Dudek, Magdalena and Tomczyk, Piotr and Wygonik, Piotr and Korkosz, Mariusz and Bogusz, Piotr and Lis, Bartłomiej. Hybrid fuel cell–battery system as a main power unit for small Unmanned Aerial Vehicles (UAV). *Int. J. Electrochem. Sci*, 8:8442–8463, 2013.

[10] Fujii, Katsuya and Higuchi, Keita and Rekimoto, Jun. Endless flyer: a continuous flying drone with automatic battery replacement. In *2013 IEEE 10th International Conference on Ubiquitous Intelligence and Computing and 2013 IEEE 10th International Conference on Autonomic and Trusted Computing*, pages 216–223. IEEE, 2013.

[11] Haddal, Chad C and Gertler, Jeremiah. Homeland security: Unmanned aerial vehicles and border surveillance. LIBRARY OF CONGRESS WASHINGTON DC CONGRESSIONAL RESEARCH SERVICE, 2010.

[12] Hayhurst, Kelly J and Maddalon, Jeffrey M and Miner, Paul S and DeWalt, Michael P and McCormick, G Frank. Unmanned aircraft hazards and their implications for regulation. In *2006 ieee/aiaa 25TH Digital Avionics Systems Conference*, pages 1–12. IEEE, 2006.

[13] Kim, Jonghoe and Song, Byung Duk and Morrison, James R. On the scheduling of systems of UAVs and fuel service stations for long-term mission fulfillment. *Journal of Intelligent & Robotic Systems*, 70(1-4):347–359, 2013.

[14] Kim, Kyunghwan and Kim, Taegyu and Lee, Kiseong and Kwon, Sejin. Fuel cell system with sodium borohydride as hydrogen source for unmanned aerial vehicles. *Journal of Power Sources*, 196(21):9069–9075, 2011.

[15] Kim, Seon Jin and Ahmadian, Navid and Lim, Gino J and Torabbeigi, Maryam. A Rescheduling Method of Drone Flights under Insufficient Remaining Battery Duration. In *2018 International Conference on Unmanned Aircraft Systems (ICUAS)*, pages 468–472. IEEE, 2018.

[16] Kim, Seon Jin and Lim, Gino J. Drone-aided border surveillance with an electrification line battery charging system. *Journal of Intelligent & Robotic Systems*, 92(3-4):657–670, 2018.

[17] Kim, Seon Jin and Lim, Gino J and Cho, Jaeyoung and Côté, Murray J. Drone-aided healthcare services for patients with chronic diseases in rural areas. *Journal of Intelligent & Robotic Systems*, 88(1):163–180, 2017.

[18] Klesh, Andrew T and Kabamba, Pierre T. Solar-powered aircraft: Energy-optimal path planning and perpetual endurance. *Journal of Guidance, Control, and Dynamics*, 32(4):1320–1329, 2009.

[19] Koslowski, Rey and Schulzke, Marcus. Drones Along Borders: Border Security UAVs in the United States and the European Union. *International Studies Perspectives*, 19(4):305–324, 2018.

[20] Kreps, Sarah E and Wallace, Geoffrey PR. International law, military effectiveness, and public support for drone strikes. *Journal of Peace Research*, 53(6):830–844, 2016.

[21] Lee, Danny and Zhou, Joe and Lin, Wong Tze. Autonomous battery swapping system for quadcopter. In *2015 International Conference on Unmanned Aircraft Systems (ICUAS)*, pages 118–124. IEEE, 2015.

[22] Lee, Jon and Leyffer, Sven. *Mixed integer Nonlinear Programming*, volume 154. Springer Science & Business Media, 2011.

[23] Gino J Lim, Laleh Kardar, and Wenhua Cao. A hybrid framework for optimizing beam angles in radiation therapy planning. *Annals of Operations Research*, 217(1):357–383, 2014.

[24] Lim, Gino J and Kim, Seonjin and Cho, Jaeyoung and Gong, Yibin and Khodaei, Amin. Multi-UAV pre-positioning and routing for power network damage assessment. *IEEE Transactions on Smart Grid*, 9(4):3643–3651, 2018.

[25] Naidoo, Yogianandh and Stopforth, Riaan and Bright, Glen. Development of an UAV for search & rescue applications. In *IEEE Africon'11*, pages 1–6. IEEE, 2011.

[26] Paucar, Carlos and Morales, Lilia and Pinto, Katherine and Sánchez, Marcos and Rodríguez, Rosalba and Gutierrez, Marisol and Palacios, Luis. Use of drones for surveillance and reconnaissance of military areas. In *International Conference of Research Applied to Defense and Security*, pages 119–132. Springer, 2018.

[27] Restas, Agoston. Drone applications for supporting disaster management. *World Journal of Engineering and Technology*, 3:316–321, 2015.

[28] Maryam Torabbeigi, Gino J Lim, and Seon Jin Kim. Drone delivery scheduling optimization considering payload-induced battery consumption rates. *Journal of Intelligent & Robotic Systems*, 97(3):471–487, 2020.

[29] Torabbeigi, Maryam and Lim, Gino J and Kim, Seon Jin. Drone delivery schedule optimization considering the reliability of drones. In *2018 International Conference on Unmanned Aircraft Systems (ICUAS)*, pages 1048–1053. IEEE, 2018.

[30] Wang, Chunjie and Ma, Zheng. Design of wireless power transfer device for UAV. In *2016 IEEE International Conference on Mechatronics and Automation*, pages 2449–2454. IEEE, 2016.

[31] Williams, Alexander and Yakimenko, Oleg. Persistent mobile aerial surveillance platform using intelligent battery health management and drone swapping. In *2018 4th International Conference on Control, Automation and Robotics (ICCAR)*, pages 237–246. IEEE, 2018.

[32] Xie, Liguang and Shi, Yi and Hou, Y Thomas and Lou, Andwenjing. Wireless power transfer and applications to sensor networks. *IEEE Wireless Communications*, 20(4):140–145, 2013.

[33] Zamichow, Nora. Marine Drones Used in Drug War. *Los Angeles Times*, 8, 1990.

Appendices

A. *E-line system on border line*

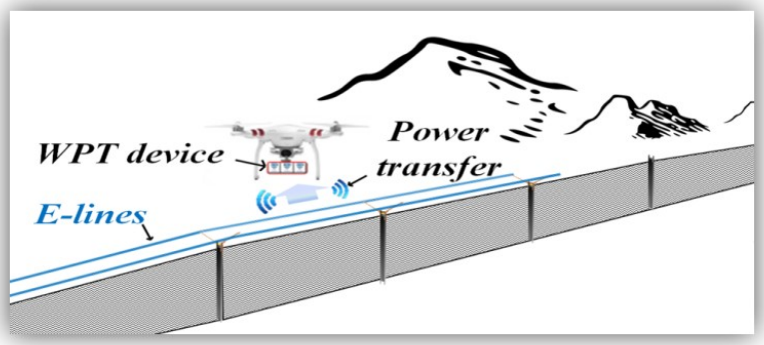

Figure 11: E-line system on border walls [16]

B. *Proof of Proposition 1*

Proof. It suffices to show that $2 \cdot max(t_\lambda, t_\mu)$ is both a lower bound and an upper bound for $\mathcal{G}_i^*$, and it is achieved by selecting the scanning pattern, in which the drone simply flies directly between E_1 and E_2 and changes the direction only at the endpoints. If a drone travels between the two endpoints E_1 and E_2 directly and continuously, for every waypoint i located in that segment, the maximum gap occurs when the drone leaves and flies to the furthest endpoint of the line and then returns. The flight time from waypoint i to the furthest endpoint of the segment is $max(t_\lambda, t_\mu)$, and the direct flight cycle between the endpoints (i.e., $p := < E_1 - E_2 - E_1 >$ or $< E_2 - E_1 - E_2 >$) is a feasible solution to the minimization of $\mathcal{G}_i^*$. Hence, $2 \cdot max(t_\lambda, t_\mu)$ is an upper bound of $\mathcal{G}_i^*$.

Without loss of generality, suppose that $\lambda_i \geq \mu_i$ for waypoint i. Let t_1 denote the most recent time the drone visited waypoint i, t_2 be the time at which the drone visits E_1 after leaving waypoint i, and t_3 be the time of the next visit at the waypoint again. There are two possible path options for the drone to travel from waypoint i to endpoint E_1: Path 1 $:= < i - E1 >$ or Path 2 $:= < i - E_2 - \cdots E_1 >$. Path 1 is the direct flight from waypoint i to E_1, and the corresponding travel time will be $t_2 - t_1 = t_\lambda$. In Path 2, the drone visits other places before heading to E_1: accordingly, $t_2 - t_1 > t_\lambda$. Therefore, $t_2 - t_1 \geq t_\lambda$ will satisfy either of the situations. Similarly, $t_3 - t_2 \geq t_\lambda$. Hence $t_3 - t_1 \geq 2t_\lambda$. This implies that the maximum revisiting gap for waypoint i is more than $2t_\lambda$. Similarly, we can prove that when $\mu_i \geq \lambda_i$, the maximum revisiting gap is more than $2t_\mu$, thus $\mathcal{G}^* \geq 2 \cdot max(t_\lambda, t_\mu)$. Since $2 \cdot max(t_\lambda, t_\mu)$ is both a lower bound and an upper bound for $\mathcal{G}^*$, we have $\mathcal{G}^* = 2 \cdot max(t_\lambda, t_\mu)$. Also, since the optimal value can be generated by flying the drone directly between E_1 and E_2 and changing the direction only at the endpoints, which is the optimal scanning pattern. □

C. E-Line Length and E-Line Passing Speed

Proposition 3. *The total E-line length is an increasing function of the drone speed while passing the E-line (i.e., $\frac{d\mathcal{L}}{dV^e} > 0$).*

Proof. According to Equation (11), to find a feasible solution to the problem, the parameters of the problem should be defined in a way that:

$$0 \leq \mathcal{L} \leq D \Rightarrow 0 \leq \frac{V^e\theta_{dis}}{\phi_e V\theta_{ch} + V^e\theta_{dis} - V\theta_{dis}} \leq 1$$

$$\Rightarrow \begin{cases} V^e\theta_{dis} \geq 0 \Rightarrow \phi_e V\theta_{ch} + V^e\theta_{dis} - V\theta_{dis} > 0 \Rightarrow (V - V^e)\theta_{dis} < \phi_e V\theta_{ch} & (.1) \\ \phi_e V\theta_{ch} + V^e\theta_{dis} - V\theta_{dis} \geq V^e\theta_{dis} \Rightarrow \phi_e V\theta_{ch} \geq V\theta_{dis} \Rightarrow \phi_e\theta_{ch} \geq \theta_{dis} & (.2) \end{cases}$$

The slope of the changes in the required total E-line length per E-line passing speed can be calculated as:

$$\frac{d\mathcal{L}}{dV^e} = \frac{d\frac{V^e\theta_{dis}}{\phi_e V\theta_{ch} + V^e\theta_{dis} - V\theta_{dis}}D}{dV^e} = D\frac{\theta_{dis}(\phi_e V\theta_{ch} + V^e\theta_{dis} - V\theta_{dis}) - \frac{d\phi_e}{dV^e}V\theta_{ch}V^e\theta_{dis} - V^e\theta_{dis}^2}{(\phi_e V\theta_{ch} + V^e\theta_{dis} - V\theta_{dis})^2} \quad (.3)$$

$$\begin{aligned} &\theta_{dis}(\phi_e V\theta_{ch} + V^e\theta_{dis} - V\theta_{dis}) - \frac{d\phi_e}{dV^e}V\theta_{ch}V^e\theta_{dis} - V^e\theta_{dis}^2 \\ &= \theta_{dis}(\phi_e V\theta_{ch} - V\theta_{dis}) - \frac{d\phi_e}{dV^e}V\theta_{ch}V^e\theta_{dis} + V^e\theta_{dis}^2 - V^e\theta_{dis}^2 \\ &= \theta_{dis}(\phi_e V\theta_{ch} - V\theta_{dis}) - \frac{d\phi_e}{dV^e}V\theta_{ch}V^e\theta_{dis} \end{aligned}$$

By Equation (.2): $\phi_e V\theta_{ch} \geq V\theta_{dis} \Longrightarrow \theta_{dis}(\phi_e V\theta_{ch} - V\theta_{dis}) - \frac{d\phi_e}{dV^e}V\theta_{ch}V^e\theta_{dis} > -\frac{d\phi_e}{dV^e}V\theta_{ch}V^e\theta_{dis}$. As stated in Section 2, reducing the speed of the drones while they pass the E-line makes drone control easier. As a result, drones are charged more efficiently. So, the efficiency function is a decreasing function of the E-line passing speed (i.e., $\frac{d\phi_e}{dV^e} < 0$). Parameters V, θ_{ch}, V^e, and θ_{dis} are all positive values, which means:

$$\begin{aligned} &-\frac{d\phi_e}{dV^e}V\theta_{ch}V^e\theta_{dis} > 0 \\ &\Longrightarrow \theta_{dis}(\phi_e V\theta_{ch} + V^e\theta_{dis} - V\theta_{dis}) - \frac{d\phi_e}{dV^e}V\theta_{ch}V^e\theta_{dis} - V^e\theta_{dis}^2 > 0 \\ &\Longrightarrow \frac{d\mathcal{L}}{dV^e} > 0 \end{aligned}$$

Because the function has a positive slope, the function is an increasing function. □